

Localization in self-affine energy landscapes

Stefanie Russ,¹ Jan W. Kantelhardt,¹ Armin Bunde,¹ and Shlomo Havlin²

¹*Institut für Theoretische Physik III, Universität Giessen, D-35392 Giessen, Germany*

²*Minerva Center and Department of Physics, Bar-Ilan University, Ramat-Gan 52900, Israel*

(Received 10 April 2001; published 12 September 2001)

We discuss the localization behavior of quantum particles in a one-dimensional Anderson model with self-affine random potentials, characterized by a Hurst exponent $H > 0$. Depending on H and energy E , a new type of “strong” localization can occur, where all states are localized in a way different from the regular Anderson localized states. Using scaling arguments, we derive an analytical expression for the phase diagram and test it by numerical calculations. Finally, we consider a somewhat related model where the variance of the potential fluctuations is kept fixed for all system sizes L and a transition between localized and apparently extended states has been reported.

DOI: 10.1103/PhysRevB.64.134209

PACS number(s): 71.23.An, 72.15.Rn, 05.40.-a

I. INTRODUCTION

In the past decades, the question of localization in disordered systems has attracted much interest (for reviews see, e.g., Refs. 1,2). In this work, we discuss, how localization is changed, when the disorder is spatially long-range correlated. We focus on one-dimensional systems and consider single-particle electronic wave functions in the tight-binding approximation. In this approximation, the Schrödinger equation becomes

$$E\psi_n = V_{n,n-1}\psi_{n-1} + \epsilon_n\psi_n + V_{n,n+1}\psi_{n+1}. \quad (1)$$

Here, E is the energy eigenvalue, $|\psi_n|^2$ is the probability to find an electron at site n , ϵ_n are the site potentials, and $V_{n,n-1} = V_{n-1,n}$ and $V_{n,n+1} = V_{n+1,n}$ are the hopping terms between nearest-neighbor sites. In the following, we concentrate on the Anderson model with diagonal disorder, where all hopping terms are set to unity and only the ϵ_n are disordered.

It had long been believed that all states of the one-dimensional Schrödinger equation in a random potential are localized exponentially.^{3,4} However, asymptotic exponential localization throughout the energy band in one dimension was rigorously proven only for completely uncorrelated random potentials.^{1,5}

Meanwhile, several systems with differing behavior have been found. Some systems with correlated disordered potentials exhibit a certain amount of extended states. Among these, we can distinguish between long- and short-range correlated potential models. An example for the latter are random-dimer models, where the local potential has a binary distribution and one of the two values (here: ϵ_A) occurs always pairwise, giving, e.g., chains with series of site energies

$$\epsilon_A, \epsilon_A, \epsilon_B, \epsilon_A, \epsilon_A, \epsilon_A, \epsilon_A, \epsilon_B, \epsilon_B, \epsilon_A, \epsilon_A, \epsilon_B, \dots \quad (2)$$

It has been theoretically predicted⁶ and numerically proven by transfer-matrix methods^{7,8} that a discrete number of the eigenstates are extended. Experimental evidence for these extended states has recently been gained by transmission measurements on random-dimer semiconductor superlattices.⁹

Extended states occur also in certain one-dimensional incommensurate systems,^{10,11} which can be viewed as systems with special long-range correlations. Here, the site energies are described by a periodic function $\epsilon_n = V(n\omega)$, whose period $2\pi/\omega$ is incommensurate with the lattice periodicity, i.e., ω is an irrational number. Most common is the Harper model,¹¹ where $V(n\omega) = (w/2)\cos(2\pi n\omega)$. In this model a localization-delocalization transition occurs. All states are extended for $w < w_c = 4$ and localized for $w > w_c$.

In Ref. 12 the inverse localization length was calculated for one-dimensional systems with stationary long-range correlated potentials, among them incommensurate systems, in an analytical perturbative approach for energies not too close to the band center or to the band edges. It was shown, how to construct site potentials ϵ_n , that lead to preset localization-delocalization transitions. The mobility edges of these systems were demonstrated experimentally by microwave transition measurements on waveguides with inserted correlated scatterers.¹³ In view of the following discussion, we would like to stress that this construction was developed for stationary potentials $\epsilon_n \ll 1$ (see below).

In this paper, we deal with another type of exception, namely with wave functions that are localized, but do not decay in an homogeneous way. We consider the Anderson model in a self-affine landscape. The aim of this paper is to elucidate the conditions leading to nonexponential localization in this case. The crucial point is that the fluctuations of self-affine systems increase with system size. Self-affine potentials are therefore nonstationary. To estimate these fluctuations, we note that the local potentials ϵ_n are given by the trace of a fractional Brownian particle with Hurst exponent $H > 0$.^{14,15} Accordingly, the fluctuations of the potential increase with increasing length scale l as

$$\langle (\epsilon_{n+l} - \epsilon_n)^2 \rangle \sim l^{2H}. \quad (3)$$

Consequently, the potential fluctuations increase with the system size.

Recently, the occurrence of a localization-delocalization transition was reported^{16,17} for a somewhat different model, where one imposes the normalization condition

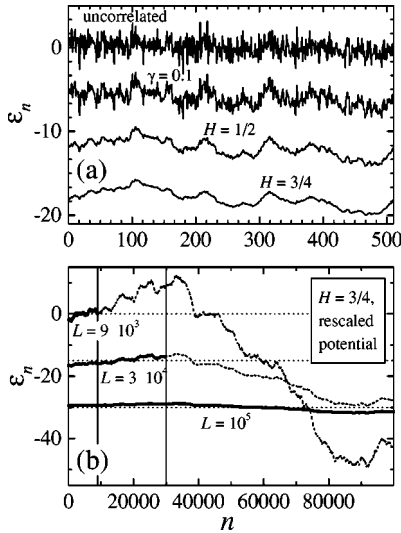


FIG. 1. Illustration of several normalized potential landscapes. In (a) four types of local potentials ϵ_n are shown: Uncorrelated random potential (top line), correlated potential with $\gamma=0.1$, and self-affine potential landscapes with $H=1/2$ and $3/4$. The correlated potential landscapes are shifted by integer multiples of 6. The curves in (b) show the same potential landscape with $H=3/4$, but rescaled such that the variance σ^2 is kept fixed ($\sigma=1$) for all system sizes considered ($L=9 \times 10^3$, 3×10^4 , and 10^5). It is obvious that for increasing system sizes the potential landscape becomes smoother due to the rescaling.

$$\sigma^2 \equiv \langle \epsilon_n^2 \rangle - \langle \epsilon_n \rangle^2 \equiv \frac{1}{L} \sum_{n=1}^L \epsilon_n^2 - \left(\frac{1}{L} \sum_{n=1}^L \epsilon_n \right)^2 = 1 \quad (4)$$

that keeps the fluctuations fixed for all system sizes L . This normalization corresponds to dividing all ϵ_n by L^H . In this case the states near the center of the band seem to become extended for $H > 1/2$. However, as the normalization condition (4) depends on the system size, the structural properties, i.e., the local smoothness of the system now become length-dependent. Larger chains are smoother than shorter chains and this is the origin for the artificial localization-delocalization transition,¹⁸ see also Ref. 19 [note Fig. 1(b), which will be discussed later].

Here, we study the problem of Anderson localization on self-affine potentials with and without renormalization. First, in Sec. II, we explain, how our self-affine chains are constructed and how the localization lengths are calculated by the transfer-matrix method. In Sec. III we consider the system without renormalization and show that a crossover towards strongly localized states occurs in this case. This crossover is accompanied by large fluctuations of the localization length. In Sec. IV, we calculate the wave functions of the strongly localized states and show that they decay non-exponentially and can thus be distinguished from the usual Anderson localization. In Sec. V, we determine the phase diagram that defines the crossover towards strongly localized states in the E - H plane analytically and confirm it by numerical simulations. Finally, in Sec. VI, we consider self-affine potentials with the additional normalization condition

(4) and calculate the phase diagram between apparently extended and localized states in this case.

II. MODEL AND METHODS

In the most common form of the Anderson model (1) with diagonal disorder, the site potentials ϵ_n are uncorrelated random numbers with zero mean, chosen randomly from a uniform distribution of width w , i.e., $\epsilon_n \in [-w/2, w/2]$. Here, w is a positive constant determining the degree of the disorder. This model has been thoroughly investigated both analytically and numerically, see, e.g., Ref. 1. The wave functions are all spatially localized in one and two dimensions for any degree of disorder. Apart from the regions near the band edges, the localization length λ scales as $\lambda(w) \sim w^{-2}$ for small w .²⁰ Accordingly, $\lambda(w)$ diverges for $w \rightarrow 0$, but for sufficiently large systems the eigenfunctions are always localized, if $w > 0$.

Less is known for the case of correlated potentials, where the correlation function $C(l) \equiv \langle \epsilon_n \epsilon_{n+l} \rangle \equiv (1/L) \sum_{n=1}^L \epsilon_n \epsilon_{n+l}$ does not vanish for $l > 0$. For long-range correlated potentials, $C(l) \sim l^{-\gamma}$, with the correlation exponent γ ($0 < \gamma < 1$), the variance σ^2 is independent of L and the series is stationary. Results from the transfer matrix method, from level statistics, and from a renormalization group technique indicate that all eigenfunctions remain localized.^{16,17,21}

Here, we focus on self-affine random potential landscapes, which may be considered having stronger correlations and can be described by a negative correlation exponent γ . They can be generated by random walks,²² Fourier transform,^{15,23} or by the random midpoint displacement method.^{14,15} The potential at site $n+1$ depends on the potential at site n by $\epsilon_{n+1} = \epsilon_n + \delta_n$, where the increments δ_n are random numbers from an interval of mean $\langle \delta_n \rangle = 0$ and fixed variance $\Delta^2 \equiv \langle \delta_n^2 \rangle$. Regarding the correlations of the increments, three cases have to be distinguished: (i) The δ_n are uncorrelated and the ϵ_n are thus essentially constructed by the trace of a random walk, i.e., ϵ_n corresponds to the displacement of a random walker after n steps. Since the mean-square displacement $\langle r^2(t) \rangle$ at time t obeys Ficks law for large t , $\langle r^2(t) \rangle \sim t$, we have $\langle (\epsilon_{n+l} - \epsilon_n)^2 \rangle \sim l$ for large l . (ii) The increments δ_n are long-range correlated with a correlation function $\langle \delta_n \delta_{n+l} \rangle \sim l^{-\gamma}$, $0 < \gamma < 1$ and the ϵ_n correspond therefore to the trace of a fractional random walk (see, e.g., Ref. 15), where $\langle r^2(t) \rangle \sim t^{2H}$ with the Hurst exponent $H = 1 - \gamma/2$, hence $1/2 < H < 1$. Case (i) corresponds to an Hurst exponent of $H = 1/2$. Landscapes with Hurst exponents $H > 1$ can be obtained by successive summations, using the resulting potentials of the previous random walk as the increments of the following, and so on. Each new summation will increase the Hurst exponent by 1. (iii) The increments δ_n are long-range anticorrelated, which means that sections of increments with positive mean $(1/m) \sum_{i=n}^{n+m-1} \delta_i > 0$ are most likely to be followed by sections of increments with negative mean $(1/m) \sum_{i=n+m}^{n+2m-1} \delta_i < 0$ for all section sizes m . In this case the potentials ϵ_n correspond to the trace of a fractional random walk with $0 < H < 1/2$. For all positive H , the series are non-stationary and the fluctuations increase

with increasing system size L according to Eq. (3). Figure 1(a) shows, for illustration, potential landscapes for uncorrelated systems (Anderson model), for correlated systems with $\gamma=0.1$, and for self-affine systems with $H=\frac{1}{2}$ and $H=\frac{3}{4}$.

In the following we consider two models. In the first model, the variance Δ^2 of the increments δ_n is kept fixed and represents a measure for the *local* fluctuations. In contrast, the variance

$$\sigma^2 \sim \langle (\epsilon_{n+L} - \epsilon_n)^2 \rangle \sim L^{2H} \quad (5)$$

[see Eq. (3)] is a measure for the *global* fluctuations of the system and increases with increasing system size L . In the second model, σ^2 is kept constant by imposing the normalization condition (4), which is equivalent to dividing the local potentials by L^H ,

$$\epsilon_n \rightarrow \frac{\epsilon_n}{L^H}. \quad (6)$$

Figure 1(b) demonstrates that this rescaling smoothens the sequences considerably for larger systems. If the sequences are generated by the Fourier transform method^{15,23} (as done in Refs. 16,17), the rescaling is implicitly contained in the normalization factors.

In order to determine the localization behavior of the eigenstates of Eq. (1), we computed the localization lengths $\lambda(E)$ directly, following the well-known transfer-matrix method.^{1,24} In the transfer-matrix algorithm, one writes Eq. (1) as recursion equation in matrix form

$$M_n \begin{pmatrix} \psi_n \\ \psi_{n-1} \end{pmatrix} = \begin{pmatrix} \psi_{n+1} \\ \psi_n \end{pmatrix}, \quad M_n = \begin{pmatrix} E - \epsilon_n & -1 \\ 1 & 0 \end{pmatrix}. \quad (7)$$

The inverse localization length is defined by

$$\lambda(E)^{-1} = - \lim_{L \rightarrow \infty} \frac{1}{L} \ln \left| \frac{\psi_L}{\psi_0} \right|, \quad (8)$$

where $|\psi_L/\psi_0|$ can be obtained for large L from the smallest of the two eigenvalues of the product matrix

$$M^L = \prod_{n=1}^L M_n. \quad (9)$$

Hence, by diagonalizing M^L , we obtain both eigenvalues and thus the localization length λ . The λ obtained this way may fluctuate very strongly for different configurations. Therefore, in order to obtain the λ for a given energy E , we averaged λ for $N=10^4$ configurations ν by different average procedures

$$\lambda_{\text{typ}} \equiv \exp \left[\frac{1}{N} \sum_{\nu=1}^N \ln \lambda^{(\nu)} \right], \quad (10)$$

$$\lambda_{\text{Lyap}} \equiv \left[\frac{1}{N} \sum_{\nu=1}^N (\lambda^{(\nu)})^{-1} \right]^{-1}, \quad (11)$$

and

$$\lambda_{\text{arith}} \equiv \frac{1}{N} \sum_{\nu=1}^N \lambda^{(\nu)}. \quad (12)$$

We define the corresponding relative fluctuations $\delta\lambda$ of the localization lengths by

$$\delta\lambda_{\text{typ}} \equiv \exp \left\{ \left[\frac{1}{N} \sum_{\nu=1}^N \ln^2 \lambda^{(\nu)} - (\ln \lambda_{\text{typ}})^2 \right]^{1/2} \right\}, \quad (13)$$

$$\delta\lambda_{\text{Lyap}} \equiv \left[\frac{1}{N} \sum_{\nu=1}^N (1/\lambda^{(\nu)})^2 - (\lambda_{\text{Lyap}})^{-2} \right]^{1/2} \lambda_{\text{Lyap}}, \quad (14)$$

and

$$\delta\lambda_{\text{arith}} \equiv \left[\frac{1}{N} \sum_{\nu=1}^N (\lambda^{(\nu)})^2 - (\lambda_{\text{arith}})^2 \right]^{1/2} \frac{1}{\lambda_{\text{arith}}}. \quad (15)$$

As we will see in the following, these fluctuations show large maxima at transition and crossover points between states of different localization behavior and we will use the maxima as indicators for the positions of these points. The same method has been used to determine the transition points in the context of electronic wavefunctions in 1D random periodic-on-average systems by Deych *et al.*²⁵

To get more information about the localization behavior, it is useful to determine not only the localization lengths and their fluctuations but also to calculate some of the eigenfunctions of Eq. (1) with diagonal disorder. We have used an iteration procedure,²⁶ which we briefly describe now. We consider a chain of $2L'+1$ sites ($n=-L', \dots, 0, \dots, L'$) with periodic boundary conditions. Starting with an initial value for the energy E , we define the coefficients $a_{-1}=E-\epsilon_{-1}$, $a_0=1$, and $a_1=E-\epsilon_1$, and recursively set

$$a_n = (E - \epsilon_n) a_{n-1} - a_{n-2}, \quad (16)$$

$$a_{-n} = (E - \epsilon_{-n}) a_{-(n-1)} - a_{-(n-2)} \quad (17)$$

for $n=2, \dots, L'$. Using these coefficients, Eq. (1) can be recursively rewritten to become

$$\psi_0 = a_n \psi_n - a_{n-1} \psi_{n+1} = a_{-n} \psi_{-n} - a_{-(n-1)} \psi_{-(n+1)} \quad (18)$$

for $n=1, \dots, L'$. For $n=L'$, the periodic boundary conditions $\psi_{L'+1} = \psi_{-L'}$ and $\psi_{-(L'+1)} = \psi_{L'}$ can be inserted, and after setting the starting value $\psi_0=1$, $\psi_{L'}$ and $\psi_{-L'}$ can be calculated. Using these results, all ψ_n and ψ_{-n} can be calculated recursively for $n=L'-1, \dots, 1$ using Eq. (18). By this procedure, (yet unnormalized) results for all ψ_n , $n=-L', \dots, 0, \dots, L'$ are obtained. Since we use an odd number of lattice sites, the only equation that still might not be fulfilled is Eq. (1) for $n=0$ [not included in Eq. (18); again with $\psi_0=1$]:

$$\epsilon_0 + \psi_{-1} + \psi_1 - E = 0. \quad (19)$$

This equation is only fulfilled if our starting value for E is an eigenvalue. Hence, by varying the starting value for E successively until Eq. (19) is fulfilled, we arrive at an eigen-

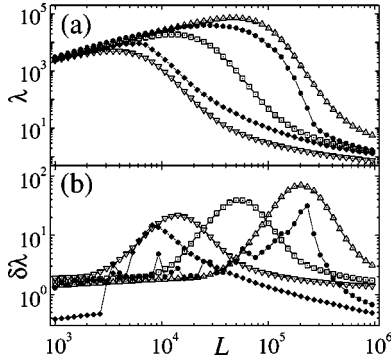


FIG. 2. System size dependence of (a) the localization lengths λ and (b) its fluctuations $\delta\lambda$ for self-affine potential landscapes with $H=1/2$ that have been generated by summing uncorrelated random numbers with different variances Δ^2 . The calculations were performed by the transfer matrix method at $E=0.5$ (close to but not directly at the band center) for 10^4 configurations. The symbols indicate: typical averages [Eqs. (10),(13)] for $\Delta=0.005$ (\triangle), $\Delta=0.01$ (\square), and $\Delta=0.02$ (∇); arithmetic average [Eqs. (12),(15)] for $\Delta=0.01$ (\bullet); Lyapunov average [Eqs. (11),(14)] for $\Delta=0.01$ (filled diamonds).

value E and an eigenfunction ψ_n , $n = -L', \dots, 0, \dots, L'$, which is normalized in the last step (eliminating the arbitrary choice $\psi_0 = 1$).

III. STRONGLY LOCALIZED STATES: LOCALIZATION LENGTH AND FLUCTUATIONS IN NONRESCALED SELF-AFFINE ENERGY LANDSCAPES

For our numerical studies we first consider nonrescaled self-affine potential landscapes generated by the random walk method,²² where the fluctuations σ^2 of the potential landscapes increase with L according to Eq. (5). We first show in Fig. 2, how the system-size dependent localization length $\lambda(L)$ and its fluctuations $\delta\lambda$ behave close to the band center. We calculated $\lambda(L)$ for different variances Δ^2 of the increments and for the different averaging procedures of Eqs. (10)–(12). The localization behavior of the eigenstates can be deduced from the dependence of $\lambda(L)$ on the system size L . For delocalized states [with $\lambda(\infty) \gg L$], $\lambda(L)$ increases linearly with L , whereas, for localized states (in the usual Anderson model) it approaches a constant value for $L \rightarrow \infty$. Note that the possible variety of scaling behaviors is more rich in the case of rescaled potentials (see Sec. VI).

Figure 2(a) shows for fixed energy $E=0.5$, how the localization lengths $\lambda(L)$ behave with increasing system size L in our case. For small L , $\lambda(L)$ increases approximately linearly with L , indicating delocalized states. Contrary to the behavior in the usual Anderson model, $\lambda(L)$ does not cross over to a constant value for large L , but drops sharply, after having reached a maximum value. The drop occurs when the system size L exceeds a limit value l that depends sensitively on Δ , H , and E , as well as on the averaging procedure. The value of l will be derived in Sec. IV. For $L > l$, $\lambda(L)$ decreases monotonously with L . At L values much larger than all relevant length scales in the system, the decay becomes smoother and the localization length λ becomes several or-

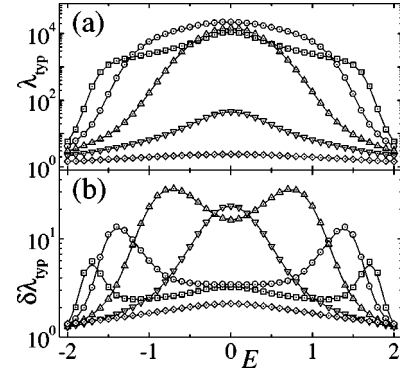


FIG. 3. Plot of (a) the typical localization length λ_{typ} [Eq. (10)] and (b) its fluctuations $\delta\lambda_{\text{typ}}$ [Eq. (13)] versus the energy E for potential landscapes with $H=1/2$ for five system sizes: $L=2^{11}$ (\square), $L=2^{13}$ (\circ), $L=2^{15}$ (\triangle), $L=2^{17}$ (∇), and $L=2^{19}$ (\diamond). 10^4 configurations have been considered in the averaging procedure. The self-affine potentials have been generated by summing uncorrelated numbers δ_n with $\Delta = \langle \delta_n \rangle^{1/2} = 0.01$.

ders of magnitude smaller than the maximum. Since in this regime λ is microscopic, we expect that single parameter scaling²⁷ does not hold in the limit of infinite system size for nonrescaled self-affine systems.

This interesting behavior with *decaying* $\lambda(L)$ is in contrast to the behavior of the localization lengths in the regular uncorrelated Anderson model. Therefore, it is reasonable to investigate the fluctuations $\delta\lambda$ of the localization lengths, defined by Eqs. (13)–(15). They are shown in Fig. 2(b) for the same parameters as in Fig. 2(a). The drop of $\lambda(L)$ is accompanied by large fluctuations $\delta\lambda$, which show maxima at the inflection point of $\lambda(L)$. While the fluctuations of λ_{Lyap} and λ_{arith} show a lot of noise in the crossover regime, the fluctuations of λ_{typ} (open symbols in Fig. 2) yield smooth and symmetric curves. For very small and very large values of L the fluctuations disappear and the different averages of λ approach each other for identical Δ . In the following, we concentrate on λ_{typ} .

Figures 3(a) and 4(a) show, for $H=1/2$ and $H=3/2$, the typical localization length $\lambda_{\text{typ}}(E)$ calculated by the transfer-

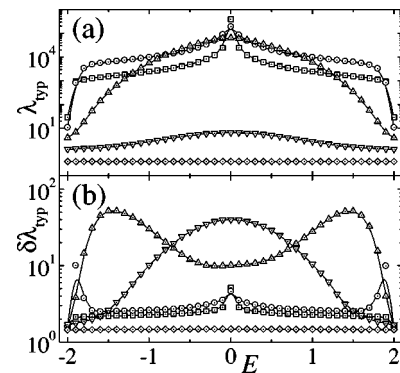


FIG. 4. Plot of (a) the typical localization length λ_{typ} and (b) its fluctuations $\delta\lambda_{\text{typ}}$ versus the energy E for potential landscapes with $H=3/2$ for five system sizes (same symbols as in Fig. 3). The potential landscapes have been generated by double summation of uncorrelated numbers δ_n with $\Delta = 5 \times 10^{-7}$.

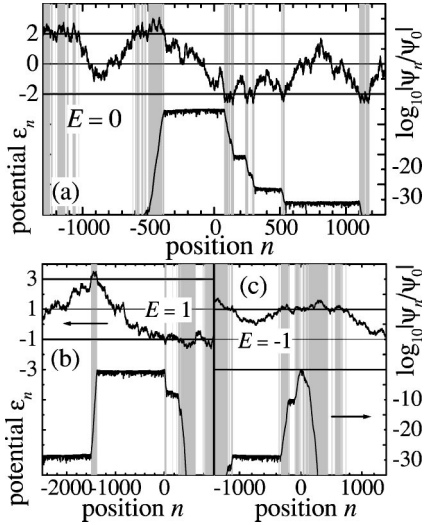


FIG. 5. Three examples of strongly localized wave functions (lower curves, right scale) with (a) $E \approx 0$, (b) $E \approx 1$, and (c) $E \approx -1$ in energy landscapes (upper curves, left scale) with $H = 1/2$, where several site energies (in the shaded regions) are larger than $E + 2$ or smaller than $E - 2$. It can be seen in all cases that these site-energies cause a sudden drop of the amplitude.

matrix method for several fixed system sizes over the whole energy range and averaged over $N = 10^4$ configurations according to Eq. (10). For small system sizes and E near the band center, $\lambda_{\text{typ}}(E)$ increases approximately linearly with L , indicating delocalized states. For large L and at the band edges, however, this behavior is reversed: $\lambda_{\text{typ}}(E)$ decreases drastically with increasing system size. We refer to the states in this regime as *strongly localized states*.

Figures 3(b) and 4(b) show $\delta\lambda$ for the same configurations as in 3(a) and 4(a), respectively. It can be clearly seen that the fluctuations have maxima at the crossover that is situated near the band edges for small system sizes L and moves to the band center for larger L . For very large system sizes, all states are strongly localized and the fluctuations of λ drop to very low values again. This enables us to determine the crossover towards strongly localized states by the maxima in the fluctuations (see also Ref. 25 and Sec. V).

IV. STRONG LOCALIZATION: WAVE FUNCTIONS

In order to determine the origin of these strongly localized states, we have investigated the explicit form of the eigenfunctions. Figure 5 shows three examples of eigenfunctions for $E \approx 0$, $E \approx 1$, and $E \approx -1$ together with the corresponding potential landscapes. Let us first look at the wavefunction with $E \approx 0$: It can be seen that the amplitude sharply drops at sites where the local potential ϵ_n exceeds a value of 2 or -2 . The drop increases drastically with increasing size of the region where the potential is outside these bounds (shaded regions in Fig. 5). With increasing system size, the fraction of sites with potentials exceeding the bound $|\epsilon_n| = 2$ increases and the wave function becomes more and more strongly localized.

For wave functions with eigenenergy $E \neq 0$ the bounds for

strong localization are shifted by E and become $|\epsilon_n - E| = 2$, as can be seen in Figs. 5(b), 5(c). Now, the wave functions drop, as soon as ϵ_n becomes larger than $2 + E$ or smaller than $-2 + E$. This behavior can be understood by the following considerations: If we apply Eq. (1) to a linear chain with all $\epsilon_n = 0$, the band of allowed eigenenergies is given by $E \in [-2, 2]$. If all local potentials are the same, $\epsilon_n \equiv \epsilon$, Eq. (1) depends only on $(E - \epsilon)$ and not on E and ϵ separately. In this case, the band is shifted to values of $[-2 + \epsilon, 2 + \epsilon]$. For fluctuating ϵ_n , we can define a local band, following the potential landscape and ranging locally from $-2 + \epsilon_n$ to $2 + \epsilon_n$. In regions, where $|\epsilon_n - E|$ exceeds 2, E is outside this local band and the respective eigenstates are strongly damped and show a sharp decay. In a very large self-affine system, where the local potentials are growing towards very large values, only strongly localized states can occur. These considerations are valid for all self-affine potential landscapes with $H > 0$. The “critical” system size, where the potential ϵ_n of one site exceeds the bound, defined by $|\epsilon_n - E| = 2$, for the first time, depends on H .

We would like to note that this strong localization behavior for self-affine potentials has to be distinguished from the usual Anderson localization, where the wave functions have an irregular structure and their amplitudes decay roughly exponentially. In contrast, in the case of strong localization, the wave functions decay practically instantaneously, when the self-affine potentials exceed the critical value. At the crossover towards strongly localized states, the potentials fluctuate between the upper and the lower bound and are thus subsequently lying above and below the critical values. As a consequence, decay regions and roughly constant regions alternate, yielding a nonexponential, patchy decay of the wave functions. From this we can understand the large fluctuations of the localization lengths in the crossover regime. We think that the usual definition of localization lengths by the Lyapunov exponent is not appropriate in this situation, because of the nonexponential decay of the wave functions. Instead, the typical (log) average and its fluctuations show a much more smooth and symmetric behavior.

A different approach may measure the size of the region, where the wave function is large. For values of $H < 1$ this can be done by random walk theory: We know that the wave functions begin to become strongly localized, when $|\epsilon_n - E|$ exceeds 2 within the system size L . The self-affine energy landscape ϵ_n can be considered as the trace of a one-dimensional random walk with the step length $\delta_n = \epsilon_n - \epsilon_{n-1}$, where the “first passage time,” i.e., the number of “steps” l required for reaching a given “distance” $\hat{\epsilon}$ scales as

$$\frac{l(\hat{\epsilon})}{A_1} = \left(\frac{A_2 \hat{\epsilon}}{\Delta} \right)^{1/H}. \quad (20)$$

Here, $\Delta \equiv \langle \delta_n^2 \rangle^{1/2}$ is the mean step length and A_1 and A_2 are nonuniversal parameters.¹⁵ Identifying $\hat{\epsilon}$ with the minimum of $2 - E$ and $2 + E$, i.e., with $2 - |E|$, we finally get

$$\frac{l(E)}{A_1} = \left(A_2 \frac{2 - |E|}{\Delta} \right)^{1/H} \quad (21)$$

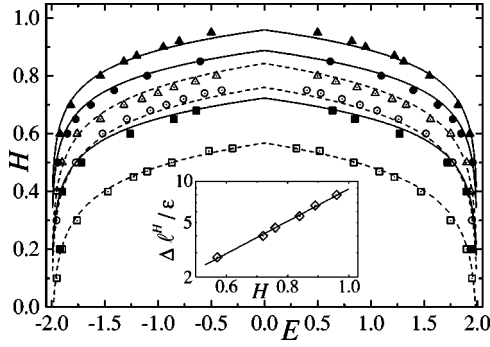


FIG. 6. Phase diagram for the Anderson model with self-affine potentials generated by Fourier transform and following single summation. The crossover towards strongly localized states, obtained from numerical simulations, is shown in the H - E plane for the following lengths L and disorder strengths Δ : $L=2^{16}$, $\Delta=0.01$ (\square), $L=2^{16}$, $\Delta=0.002$ (\odot), $L=2^{16}$, $\Delta=0.001$ (\triangle), and $L=2^{18}$, $\Delta=0.001$ (filled squares), $L=2^{18}$, $\Delta=0.0002$ (\bullet), $L=2^{18}$, $\Delta=0.0001$ (filled triangles). The theoretical curves [Eq. (22)] are included for each Δ by solid lines for $L=2^{18}$ and by dashed lines for $L=2^{16}$. To determine the parameters A_1 and A_2 , we have calculated $l(\hat{\epsilon})$ for several values of H . By plotting $\Delta l^H/\hat{\epsilon}$ versus H in a semilogarithmic scale (see inset), we obtain $A_1 = 15.2 \pm 1.0$ and $A_2 = 0.58 \pm 0.03$ by a linear fit [see Eq. (20)].

as a characteristic length scale in the self-affine systems. This relation will help to identify the crossover towards the regime of strongly localized states as shown in the following section. We would like to note that the characteristic length scale $l(\Delta, H, E)$ is distinct from the characteristic length scale l_s recently introduced by Deych *et al.* in Ref. 27 to describe the crossover to regimes where single parameter scaling is violated.

V. THE PHASE DIAGRAM IN A SELF-AFFINE ENERGY LANDSCAPE

Next we investigate how the crossover towards strongly localized states occurs. If the potentials ϵ_n reach the critical value $2 - |E|$ within the system size, the states become strongly localized. Therefore, it is obvious, that for sufficiently large values of L all states are strongly localized. For sufficiently small chains and sufficiently small values of the Hurst exponent H , on the other hand, $l(E)$ can reach the system size L (or even larger values) and strongly localized states can not occur. For fixed L , the critical lines $H(E)$ can be estimated with the help of Eq. (21). If $l(E)$ is smaller than the system size, the states are strongly localized. For a given system size L , we have therefore a critical energy E_c , where $l(E_c) = L$, that defines a crossover towards a regime of strong localization. Rearranging Eq. (21), we get

$$E_c = \pm \left[2 - \frac{\Delta}{A_2} \left(\frac{L}{A_1} \right)^H \right]. \quad (22)$$

Figure 6 shows the resulting phase diagram in the E - H plane for several values of Δ and two values of L . The symbols have been obtained by transfer-matrix calculations, investigating again the fluctuations of the localization lengths.

The remaining parameters A_1 and A_2 have been determined by separate calculations of $l(\hat{\epsilon})$, as explained in the figure caption of Fig. 6. Figure 6 shows, that the simple relationship (22) describes surprisingly well the dependence of E_c on Δ , on L and on H for self-affine potential landscapes with $H < 1$. The wave functions become strongly localized above the crossover. The critical lines are symmetric, $H(E) = H(-E)$ and the extent of the regime of strongly localized states (upper part of Fig. 6) increases with increasing Δ .

VI. THE PHASE DIAGRAM IN A RESCALED SELF-AFFINE ENERGY LANDSCAPE

Next we consider a related model of rescaled potential landscapes, suggested by de Moura and Lyra,¹⁶ where the variance σ^2 of the potentials is kept constant [see Eq. (4)]. For sufficiently large values of σ all states are strongly localized, while for sufficiently small values of σ (and sufficiently large values of H), the local fluctuations of the rescaled potentials decrease drastically, and we can expect apparent ‘‘extended’’ states [see Fig. 1(b)]. In Ref. 16, an approximate phase diagram has been determined for this apparent transition for one value of σ . According to Ref. 16, below $H=1/2$, only localized states occur.

For $1/2 < H < 1$, we can again generate the potentials by the trace of a random walk and find an analytical expression for the critical lines that separate regions of localized states from regions of apparently extended states. When the potentials are rescaled, the mean step length Δ depends on L and on the variance σ^2 by

$$\frac{\Delta}{B_2} = \sigma \left(\frac{B_1}{L} \right)^H, \quad (23)$$

where B_1 and B_2 are parameters, similar to A_1 and A_2 in Eq. (20). Inserting Eq. (23) into the relation (22), we obtain for the critical energy E_c

$$E_c = \pm \left[2 - \sigma \frac{B_1^H B_2}{A_1^H A_2} \right]. \quad (24)$$

For values of $H \geq 1$ we obtain non-stationary increments and the theoretical derivation is not valid in this case.

Figure 7 shows the resulting phase diagram in the E - H plane for several values of the variance σ^2 . In addition to the renormalization of the potentials, the numerical procedure has been the same as for Fig. 6 and again, the transition points have been determined from the maxima of the fluctuations of the localization length. Note that now the phase diagram is independent of L . The critical lines are symmetric, $H(E) = H(-E)$ and the width of the regime of ‘‘extended’’ states (near the band center for $H > 1/2$) decreases with increasing variance σ .

For Hurst exponents $H < 1$, we can compare our numerical results with the theoretical predictions of Eq. (24). The parameters A_1, A_2 are the same as in Fig. 6 and B_1, B_2 are fit parameters. The agreement between the theoretical predic-

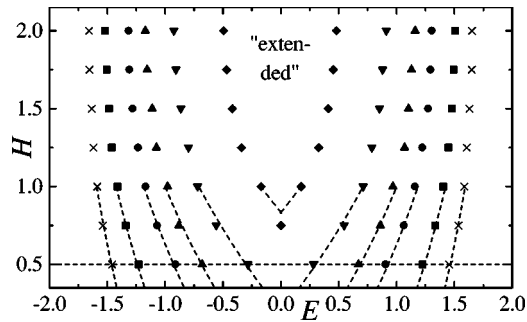


FIG. 7. Phase diagram for the Anderson model with rescaled self-affine potentials generated by Fourier transform (similar to Ref. 16). The transition from apparently extended states to localized states is shown in the H - E plane for six disorder strengths, $\sigma^2 = 0.05$ (crosses), 0.1 (boxes), 0.2 (circles), 0.3 (triangles up), 0.5 (triangles down), 1.0 (diamonds). For $H < 1$, the theoretical curves [Eq. (24)] are included in the figure for each σ (dashed lines). The parameters A_1 and A_2 are the same as in Fig. 6 and $B_1 = 8.8$ and $B_2 = 1.83$ are fit parameters. It has been verified by separate calculations that they are in the right order of magnitude. For $H < 1/2$, apparently extended states do not appear, in agreement with Ref. 16.

tion and the numerical findings for E_c is reasonable. Below $H = 1/2$, the localization lengths increase slower than the system size L .

VII. CONCLUSIONS

In conclusion, we have investigated the localization behavior of quantum particles in linear potential landscapes with self-affine random potentials, characterized by a Hurst exponent $H > 0$. In this case, the potentials are nonstationary and we found that a new type of “strong” localization can occur, as soon as the local potentials exceed the values $E \pm 2$, where E is the energy. While in the usual Anderson model, the wave functions have an irregular structure and

decay roughly exponentially, we find strong localization characterized by a patchy structure and a nonexponential decay of the wave functions. In the regime of strong localization the system-size dependent localization length *decreases* with increasing system size. This behavior is drastically different from the usual Anderson model with uncorrelated potentials, but is a universal feature of all self-affine potentials with given H independent of the way they are constructed. Indeed, the potentials always have similar properties as fractional Brownian motion and show similar universal features. Accordingly, all eigenfunctions are strongly localized, if the chains are long enough. For each finite chain of length L , we find a crossover towards strongly localized states, that depends on H and E . In this intermediate case, the usual definition of localization lengths is no longer appropriate, since the fluctuations become very large. We applied random walk theory to define a characteristic length scale $l(E)$, which describes the mean size of the region, where the patchy wave function is large. Using scaling arguments, we derived an analytical expression for a phase diagram defining (for a given chain length L) the crossover towards a regime of strongly localized states. We tested this relation for the critical lines by numerical simulations, using the transfer matrix method.

Finally, we considered a somewhat related model where the variance σ^2 of the potential fluctuations is kept fixed for all system sizes L . Recently, a localization-delocalization transition has been reported for this model for $H > 1/2$, which, however, is not a generic feature of self-affine potentials with $H > 1/2$, but due to the rescaling of the potentials. We also determined the phase diagram for this case and applied random walk theory to obtain an analytical description for $H < 1$.

ACKNOWLEDGMENTS

We would like to thank Itzhak Webman for valuable discussions and the German Israeli Foundation and the Minerva Foundation for financial support.

- ¹B. Kramer and A. MacKinnon, Rep. Prog. Phys. **56**, 1469 (1993).
- ²M. Janssen, Phys. Rep. **295**, 1 (1998).
- ³R. E. Borland, Proc. R. Soc. London, Ser. A **274**, 529 (1963).
- ⁴B. I. Halperin, Phys. Rev. A **139**, 104 (1965).
- ⁵H. Kunz and B. Souillard, Commun. Math. Phys. **78**, 201 (1980); F. Delyon, H. Kunz, and B. Souillard, J. Phys. A **16**, 25 (1983).
- ⁶D. H. Dunlap, H.-L. Wu, and P. W. Phillips, Phys. Rev. Lett. **65**, 88 (1990).
- ⁷S. N. Evangelou and E. N. Economou, J. Phys. A **26**, 2803 (1993).
- ⁸F. M. Izrailev, T. Kottos, and G. P. Tsironis, J. Phys.: Condens. Matter **8**, 2823 (1996).
- ⁹V. Bellani, E. Diez, R. Hey, L. Toni, L. Tarricone, G. B. Parravicini, F. Domínguez-Adame, and R. Gómez-Alcalá, Phys. Rev. Lett. **82**, 2159 (1999).
- ¹⁰S. Aubry and G. André, Ann. Isr. Phys. Soc. **3**, 133 (1980); A. P. Siebesma and L. Pietronero, Europhys. Lett. **4**, 597 (1987).

- ¹¹H. Hiramoto and M. Kohmoto, Int. J. Mod. Phys. B **6**, 281 (1992).
- ¹²F. M. Izrailev and A. A. Krokhin, Phys. Rev. Lett. **82**, 4062 (1999); F. M. Izrailev, A. A. Krokhin, and S. E. Ulloa, Phys. Rev. B **63**, 041102 (2001).
- ¹³U. Kuhl, F. M. Izrailev, A. A. Krokhin, and H.-J. Stöckmann, Appl. Phys. Lett. **77**, 633 (2000).
- ¹⁴J. Feder, *Fractals* (Plenum Press, New York, 1988).
- ¹⁵*Fractals in Science*, edited by A. Bunde and S. Havlin (Springer-Verlag, Heidelberg, 1994).
- ¹⁶F. A. B. F. de Moura and M. L. Lyra, Phys. Rev. Lett. **81**, 3735 (1998).
- ¹⁷F. A. B. F. de Moura and M. L. Lyra, Physica A **266**, 465 (1999).
- ¹⁸J. W. Kantelhardt, S. Russ, A. Bunde, S. Havlin, and I. Webman, Phys. Rev. Lett. **84**, 198 (2000).
- ¹⁹F. A. B. F. de Moura and M. L. Lyra, Phys. Rev. Lett. **84**, 199 (2000).

- ²⁰M. Kappus and F. Wegner, *Z. Phys.* **45**, 15 (1981).
- ²¹St. Russ, J. W. Kantelhardt, A. Bunde, S. Havlin, and I. Webman, *Physica A* **266**, 492 (1999).
- ²²In a random walk generation, we sum up previously generated uncorrelated or correlated random numbers δ_m (for $H=1/2$ or $H>1/2$, respectively) to obtain the potentials $\epsilon_n = \sum_{m=1}^n \delta_m$. The series ϵ_n is characterized by the Hurst exponent $H=1-\gamma/2$, if the δ_n were correlated with exponent γ .
- ²³H. A. Makse, S. Havlin, M. Schwartz, and H. E. Stanley, *Phys. Rev. E* **53**, 5445 (1996).
- ²⁴B. Derrida, K. Mecheri, and J. L. Pichard, *J. Phys. (Paris)* **48**, 733 (1987).
- ²⁵L. I. Deych, D. Zaslavsky, and A. A. Lisyansky, *Phys. Rev. Lett.* **81**, 5390 (1998).
- ²⁶H. E. Roman and C. Wiecko, *Z. Phys. B: Condens. Matter* **62**, 163 (1986).
- ²⁷L. I. Deych, A. A. Lisyansky, and B. I. Altshuler, *Phys. Rev. Lett.* **84**, 2678 (2000).